Energy 294 (2024) 130420

Contents lists available at ScienceDirect

Energy

journal homepage: www.elsevier.com/locate/energy

WiSOM: WiFi-enabled self-adaptive system for monitoring the occupancy in smart buildings

Muhammad Salman [a], Lismer Andres Caceres-Najarro [b], Young-Duk Seo [c], Youngtae Noh [d,*]

[a] Department of Computer & Software Engineering, College of Electrical & Mechanical Engineering, NUST, Islamabad, Pakistan
[b] Energy AI, Korea Institute of Energy Technology (KENTECH), Naju-si, Republic of Korea
[c] Department of Computer Science and Engineering, Inha University, Incheon, Republic of Korea
[d] Department of Data Science, Hanyang University, Seoul, Republic of Korea

ARTICLE INFO

Keywords:
Building energy saving (BES)
Channel state information (CSI)
Access point (AP)
Occupancy monitoring
Multipath effect
Activity of daily living
Area Of Interest (AOI)

ABSTRACT

There has been extensive research on building energy saving (BES), which aims to reduce energy consumption inside buildings. One of the key solutions for energy saving in buildings is to reduce energy consumption in areas that are not occupied by inhabitants. However, effective monitoring of occupants for energy-saving purposes can be challenging due to unpredictable variations in the indoor environment, such as variations in space size, furniture arrangement, the nature of occupants' activities (*e.g.*, varied intensities and instances), and penetration losses of walls. Unfortunately, the existing solutions for occupancy monitoring in smart buildings, such as PIR sensors, CO_2 sensors, and cameras, etc., are expensive, require excessive maintenance, and are not adaptable to the complex variations in indoor environments. This paper introduces *WiSOM*, for occupancy detection that utilizes the channel state information (CSI), of commodity WiFi. The method is self-adaptive and designed to handle complex variations in indoor environments. We conducted a thorough analysis of *WiSOM* and evaluated it under various indoor conditions, including the impact of multipath effects, the detection of different intensities and instances of activities of daily living (ADL), and the impact of wall absorption in a real-home scenario. Our evaluation demonstrated an average detection rate of 98.25% for multipath effects, 96.5% and 98.1% for different intensities and instances of ADL, and 94.4% for wall absorption. Additionally, we assessed *WiSOM*'s resilience to temporal variation in the CSI and achieved a false alarm rate of less than 2%. In comparison to recent baselines, *WiSOM* outperformed, achieving up to a 21% improvement in detection rate within real-house scenarios.

1. Introduction

The world's population is tremendously increasing and it is projected that by the year 2100 the expected population would be 10.4 billion [1]. Such a rapid growth in population would introduce two major concerns for the humans, namely, the shortage of land and run-out energy resources. The land demand can be coped with the vertical construction (*i.e.*, buildings) to accommodate a higher population density. However, the energy depletion is a serious issue, and the energy resources must be efficiently utilized to extend its run-out period.

The existing urbanized regions of the world have already adopted living in the buildings. In order to enhance the inhabitants living standard, modern buildings are installed with heating, ventilation, and air conditioning (HVAC) systems, lighting systems, and systems for supplying hot water, *etc.* Because of these living comfort services, the buildings consume the highest proportion of the total energy (i.e., around 40%) [2]. Unfortunately, building comfort services are inefficiently administered, exacerbating the waste of energy resources [3]. For instance, maintaining a thermal comfort level for a vacant apartment or office potentially waste a considerable amount of energy resources. According to a report by MIT, around 30% of the energy consumed by buildings goes wasted [4].

To prevent the waste of energy in smart buildings, several approaches have been introduced for occupancy monitoring. These approaches ensure the provision of adequate energy only to those areas where the occupants are present, whilst limiting the usage of energy in the unoccupied areas. The effective implementation of occupancy monitoring not only enhances the energy efficiency of individual buildings but also contributes to a substantial improvement in the energy flexibility of entire building clusters [5]. Recently, a couple of systems have been introduced in smart buildings for occupancy monitoring,

* Corresponding author.
E-mail addresses: msalman@ceme.nust.edu.pk (M. Salman), andrescn@kentech.ac.kr (L.A. Caceres-Najarro), mysid88@inha.ac.kr (Y.-D. Seo), youngtaenoh@hanyang.ac.kr (Y. Noh).

https://doi.org/10.1016/j.energy.2024.130420
Received 8 August 2023; Received in revised form 22 November 2023; Accepted 19 January 2024
Available online 20 January 2024
0360-5442/© 2024 Elsevier Ltd. All rights reserved.

Nomenclature

CO_2	Carbon dioxide
ADL	Activities of Daily Living
AOI	Area of Interest
AP	Access Point
BES	Building Energy Saving
BiLSTM	Bidirectional Long Short-Term Memory
CNN	Convolutional Neural Network
CSI	Channel State Information
DR	Demand Response
DWT	Discrete Wavelet Transform
EV	Electric Vehicles
GUI	Graphical User Interface
HVAC	Heating, Ventilation, and Air Conditioning
IoT	Internet of Things
IP	Internet Protocol
LoS	Line-of-Sight
MAD	Median Absolute Difference
MIMO	Multiple Input, Multiple Output
NLoS	Non-Line-of-Sight
OFDM	Orthogonal Frequency Division Multiplexing
PCA	Principal Component Analysis
PIR	Passive infrared
RPi	Raspberry Pi
RSSI	Received Signal Strength Indicator
SVM	Support Vector Machine
TV	Television
UDP	User Datagram Protocol
WiSOM	WiFi System for Occupancy Monitoring
WLAN	Wireless Local Area Network
WSN	Wireless Sensor Networks

namely Passive infrared (PIR) sensors, environmental sensors (*e.g.*, CO_2, humidity, and temperature sensor), cameras, and WiFi. The Passive Infrared (PIR) sensor is a cost-effective and power-efficient solution for occupancy monitoring in small indoor environments [6,7], but it becomes inefficient in large spaces [8]. Moreover, its sensitivity reduces with the increase in temperature [9], and it cannot detect individuals in Non-Line-of-Sight (NLoS) conditions [10]. Environmental sensors such as CO_2 sensors are more robust for monitoring large numbers of occupants [11,12], but they cause delays in reporting the presence of a single occupant [13]. Additionally, these sensors have a higher maintenance cost [14]. The surveillance camera has also been used for occupancy monitoring, and has been effective for finding the occupants [15–18]. However, camera-based solutions raise privacy concerns and is not feasible for monitoring the interior of private spaces such as homes or offices.

More recently, the widespread use of WiFi infrastructure in commercial and residential buildings has made the WiFi-based sensing approaches more popular for occupancy monitoring [19–24]. The main advantage of WiFi-based occupancy sensing techniques is their ability to be deployed to any WiFi-enabled IoT device with a few modifications to its WLAN driver, which means they do not require a dedicated device. Additionally, they passively measure occupancy, meaning they do not require active participation from the occupants and do not violate privacy concerns. In this paper,[1] we introduce a system supported by any WiFi-enabled IoT device referred to as *WiSOM*[2] to smartly sense the occupancy of the area of interest (AOI). However, unlike the existing WiFi-based occupant sensing technique which underestimates the complex indoor settings of the smart spaces (*e.g.*,smart buildings or smart homes), such as variation in size of the AOI, scatters (e.g., furniture) arrangement, intensities of occupant activities, random instances of activities of daily living (ADL), temporal variation in the CSI, and multiple wall occlusion; *WiSOM* is self-adoptive to all these complex variations in the target environment. We resolved these challenges as follows:

Variations in the indoor environment: The indoor space has varied sizes and furniture arrangements. These factors cause different multipath effects which results in false occupancy results. Thus supervised machine learning methods could not work effectively in such settings. To handle this, we introduce an unsupervised machine leaning method based on the DBSCAN algorithm [26] and in conjunction with the control chart method [27]. We adopt a self-adaptive feature to the DBSCAN method, which automatically adjusts its threshold to the variations in indoor environments.

Randomness of the occupants' activity: Understanding the behaviors of occupants in buildings is a challenging task as the intensities and instances of their ADL are inherently unpredictable and random [28,29]. The intensity refers to how vigorously an activity has been performed, and the instance refers to when the user's behavior was sedentary and when it was dynamic. To address this challenge, we leverage the kneedle method [30] for automatically finding the bifurcation point between the static and dynamic instances. This enables the adaptation of DBSCAN to activities of any intensity. In addition to that, we introduce a method for fine-tuning the estimated parameter (determined by the kneedle) to discriminate the individual's ADL of any instance accurately.

Temporal variations in CSI: The CSI data experience variations over time even if there is no activity in the AOI [31]. Such variations are due to jitter caused by surrounding traffic, building materials, and frequent small changes in the indoor environment. To tackle this, our model first identifies the static cluster, and then periodically sets the threshold of the control chart method. Thus, regardless of these temporal variations in the CSI, *WiSOM* accurately detects the presence of an occupant.

Occupant behind walls: Detecting the activity of an individual behind single or multiple walls (*i.e.*, in NLoS) using CSI is a challenging task due to the complex propagation environment and attenuation of the wireless signals. To deal with this, we apply a filter based on wavelet analysis, *i.e.*, discrete wavelet transform (DWT) [32,33]. This filter mitigates the noises caused by the complex propagation environment and preserves the Doppler frequencies that correspond to the ADL.

Based on our in-depth review presented in Section 2, focusing on both WiFi and sensor-based technologies, we discover that most existing solutions are geared towards coarse-grained occupant detection, including zone-based, RSSI-based, and scenario-specific CSI-based methods. In addition, there is a significant gap in developing self-adaptive systems that are capable of effectively detecting occupants, in spite of the complex variations found in indoor settings. To address these gaps, our paper makes three key contributions:

- We adopted CSI to overcome the limitations of existing occupancy monitoring solutions (e.g., PIR, CO_2 sensor *etc.*.) used in complex indoor environments with unforeseeable variables such as Non-Line-of-Sight scenarios and variable room sizes. To enable CSI to function effectively in complex indoor environments, we

[1] As a continuation of my previous work, I would like to acknowledge that I presented the initial idea in my conference paper titled *WiFi-enabled Occupancy Monitoring in Smart Buildings with a Self-Adaptive Mechanism*, which was published in "ACM SAC in March 2023" [25].

[2] *WiSOM* stands for **Wi**Fi **S**ystem for **O**ccupancy **M**onitoring.

conducted a process of sanitization in which we eliminated CSI's noisy subcarriers. In-band noises were subsequently filtered using discrete wavelet analysis. By then extracting the first principal component feature from the amplitude term of the filtered CSI, the occupancy (or non-occupancy) states present in the CSI were stabilized.

- To achieve the system's self-adaptability, first, we developed a novel technique for auto-estimating and fine-tuning the DBSCAN parameters. After that, we use a synergistic model that incorporates the auto-tuned DBSCAN and control chart technique; wherein the autotuned DBSCAN operates in batch mode and updates the control chart threshold in accordance with the environmental variations.
- To evaluate *WiSOM*'s performance in real-life scenarios, we build a realistic testbed based on raspberry pi-3 (*RPi 3*). We deliver the results for the aforementioned challenges, namely, rooms of different sizes with uncontrolled furniture arrangement to examine *WiSOM*'s reliability in multipath rich environments, detecting ADL with diverse intensities and instances, robustness to CSI's temporal variation over different periods, and detecting activity behind wall(s).

2. Related work

Recently, WiFi based occupancy monitoring in smart buildings has gained considerable popularity owing to ubiquitous wireless networks and massively available WiFi-enabled IoT. In the following, recent solutions for building's occupancy monitoring has been discussed. They are broadly categorized into two parts, as detailed below

2.1. Non-WiFi occupancy detection solutions

These solutions for occupancy detection include the utilization of cameras, dedicated sensors, or a hybrid combination thereof. We discuss them in detail as follows:

Camera-based occupancy monitoring. Such solutions utilize cameras for AOI monitoring and employs computer vision for occupant detection. Cui et al. employed a camera based approach consisting of their three-module [15]: Module A for occupancy detection using a camera, Module B to manage outdoor air intake based on detected occupants, and Module C for efficient airflow distribution to ensure suboptimal thermal comfort. Another work proposed by Saffari et al.. introduced a novel approach harnessing energy from ambient light for a battery-free camera system [16]. They utilized YOLOv5 [34], a computer vision algorithm, for occupancy detection across various areas within the building, showcasing the versatility of their energy-efficient occupancy detection solution. Similarly, Hu et al. introduced a building occupancy detection system using CCTV cameras, employing a deep-learning approach. This method accurately predicts both the number of occupants and their respective locations within the building [17].

Dedicated sensors based Occupancy monitoring. In this category, dedicated sensors such as temperature sensors, infrared sensors *etc.*, are used to detect the occupancy. Jin et al. utilized CO_2 sensor, and employs a mathematical model called Sensing by Proxy (SbP) paradigm, which is using partial and ordinary differential equations. This approach enables quick responses to changes in occupancy, facilitating real-time control of indoor environments [11]. Similarly, Cali et al. propose an occupancy detection system based on CO_2 concentration [12], utilizing a mass balance equation to compare occupant-generated CO_2 contributions with the known CO_2 profile of the room. Their evaluation includes scenarios with and without air conditioning in the area of interest (AOI). Dodier et al. utilize PIR sensors for real-time occupancy data collection and streaming those information to a server every second. They leverage belief network analysis, which makes real-time inferences about occupancy patterns in indoor environments [7].

Occupancy monitoring with multimodal input. Mahmud et al. employ a system with wireless sensors and cameras for occupancy detection [35]. The system updates occupant count and locations, transmitting this information wirelessly to a central server equipped with a GUI, which then makes decisions to adjust air conditioner set points and control lights based on occupancy. Han et al. presented an occupancy detection method based on the data acquired from six different sensors, including, passive infra-red (PIR) sensors, Carbon Dioxide (CO_2) concentration sensors, and relative humidity (RH) sensors. They employed Autoregressive Hidden Markov Model (ARHMM) and achieved a detection accuracy of approximately 80% [36]. Piselli et al. used Wireless Sensor Network (WSN) system to monitor occupants in five office rooms, recording parameters such as air temperature, illuminance, and appliance usage [29]. Based on the data acquired from WSN a predictive model for occupancy patterns was developed.

To sum up, non-WiFi occupancy detection solutions come with certain limitations. While camera-based solutions provide higher accuracy, their adoption within homes and offices is hindered by privacy concerns among users. Dedicated sensors also face challenges, with sensitivity affected by the distance between sensors and occupants [12]. Additionally, solutions using multiple sensors encounter practical issues, such as high computational demands and data transportation challenges to predict occupancy states on the server.

2.2. WiFi-based occupancy detection solutions

We categorize WiFi-based occupancy detection solutions into three main parts: utilizing WiFi association logs for occupancy detection, monitoring changes in WiFi signal strength (RSSI), and monitoring changes in CSI resulting from the occupant's motion in the AOI. The details are discussed below.

WiFi association based occupancy monitoring: There are numerous solutions where the occupancy is detected based on the knowledge of users association to the WiFi installed in the AOI. Balaji et al. proposed a system called *Sentinel* [37], where on the user side, they installed an application on their phone for consistently sending packets to the access point (AP). On the AP side, the received packets were identified via WiFi logs. The authors of *Sentinel* partitioned the building in *zone of detection*, where each zone was corresponding to the coverage area of a particular AP. The occupancy in *zone of detection* was anticipated via user-AP association logs [37]. Another similar work called *WiFiMon* has been proposed by Cecchet et al. The authors predict the occupancy pattern in buildings equipped with enterprise wireless networks by leveraging the WiFi logs of packets exchange between the user and AP [38]. Similarly, Trevidi et al. proposed *isschedule* system for leveraging the user-AP association information for training a machine learning model and based on that deriving the HVAC schedule. All the aforementioned system requires the installation of an application on the user side and maintaining the WiFi logs on the analytic platform. Moreover, such occupancy localization information are coarse-grained and not very accurate (*i.e.*, WiFi provides the associated user information who could be in any possible room in that area).

RSSI-based passive sensing: Another popular metric used for occupancy detection is the WiFi's received signal strength indicator (RSSI), which in particular is the power measurement between the transmitter and receiver pair. Depatla et al. exploited the RSSI for occupancy detection by leveraging the blocking of line-of-sight (LoS) between the WiFi transmitter and receiver pair, and the scattering effect from people reflection [39]. The authors used these two pieces of information, and based on the level of RSSI degradation, their framework predicted the occupancy. Longo et al. also leveraged the RSSI information for estimating the occupancy in the AOI [40]. The authors transmitted

the occupancy related data from the AOI to their web-based platform which incorporates a trained supervised machine learning model. Based on testing the occupancy data (*i.e.*, RSSI), their platform predicted the presence of occupants. Similarly, Xu et al. profiled the environment by fingerprinting method, and predicted the location of the occupant based on multiple RSSI transmitters and receivers [41]. Retrieving and processing RSSI measurements are straightforward and computationally efficient for both localization and occupancy detection. However, the RSSI is susceptible to background noises and temporal variations, making it less reliable. Additionally, it is highly affected by multipath effects [42]. Therefore, approaches based on RSS measurements for detecting occupancy are prone to higher errors [43].

CSI-based passive sensing: The CSI, as opposed to the RSSI, characterizes small-scale multipath fading, making it a more precise descriptor of the wireless channel. Thus, the fine grained information contained in the CSI enables accurate estimation of occupants in the AOI. The CSI-based endeavors for occupancy detection in smart buildings are discussed below:

Yang et al. proposed cloud based occupancy monitoring platform. The authors transmitted the collected CSI data to the cloud server via MQ telemetry transport protocols. The cloud server incorporates a machine learning algorithm, which forecasts the state of occupancy based on the CSI data [21]. Soltanaghaei et al. proposed an occupancy detection solution based on analyzing the multipath reflections of the CSI. They treat each multipath a separate sensor. In doing so, they are able to distinguish the highly fluctuating multipath that corresponds to the reflection from the moving occupants in the target area [22]. Lastly, in some works the algorithms for detecting the occupancy compare the shape similarity between nearby time series CSI data [19,20].

In summary, the existing CSI based solutions provide extensive details on how to detect the occupants in a particular controlled environment. However, they lacks the focus on uncontrolled environmental factors such as changing the size and scatters in the target environment, varying the intensity and instances of ADL, considering the temporal variations in CSI, and multiple wall occlusion (*i.e.*, occupants in non-line-of-sight). These factors highly affect the performance of the occupancy detector. In this work, we leverage the CSI of commodity WiFi signals and propose a self-adaptive occupancy detection system to such complex variations in indoor environments.

3. Methodology

When a WiFi signal travels from a transmitter to a receiver, it can be affected by various factors, including reflections, refraction, and scattering. These effects cause the signal to take multiple paths and arrive at the receiver at different times, resulting in a phenomenon called multipath. When the signal is degraded due to multipath, the CSI retains information about the degree to which the channel was degraded [44]. These details are given at the granularity of the orthogonal frequency-division multiplexing (OFDM) subcarriers. The presence of occupants in the AOI additionally disrupts the WiFi propagation channel, resulting in larger variations in CSI. Exploiting this phenomenon can assist us in determining the movement of occupants in that area. However, raw CSI data cannot be directly used for occupancy detection due to the presence of short spikes, zero bins, and noise. Thus, the raw CSI data must be cleaned and preprocessed beforehand. Subsequently, we elaborate on the particulars of our methodology, which are illustrated in Fig. 1.

3.1. CSI sanitization

First, the CSI data for the AOI is collected and the noisy subcarriers are removed as follows.

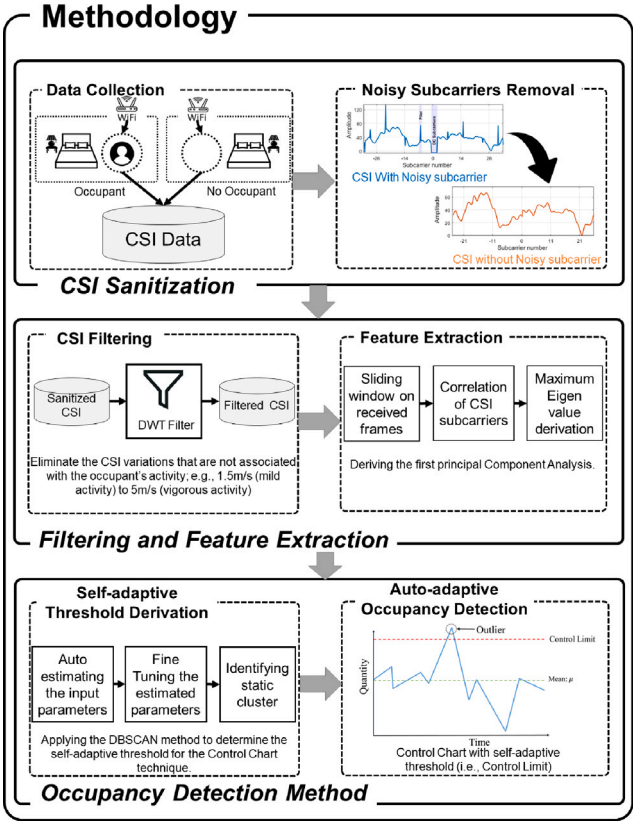

Fig. 1. High-level overview of the occupancy detection methodology.

Removal of noisy subcarriers

The number of subcarriers in the received frames depends on the channel bandwidth. Specifically, frames with bandwidth of 20 MHz, 40 MHz, 80 MHz, and 160 MHz, respectively, have 64, 114, 242, and 484 subcarriers [45]. There are three different CSI subcarrier types present inside the data frames: the pilot subcarriers, used to monitor variations in frequency, amplitude, and phase; the data subcarriers, used to transport the modulated data; and the DC (or null) subcarriers act as a guard carrier and do not carry any information, but are instead used to prevent interference with neighboring channels. As an example, in the 802.11n/ac standard with a channel bandwidth of 20 MHz, there are 64 CSI subcarriers in total, where 52 subcarriers are allocated for data, 8 for pilot subcarriers, and the remaining 4 for DC/null subcarriers that act as guard carriers to avoid interference with neighboring channels. The DC and pilot subcarriers have asymmetric shapes as opposed to data subcarriers. The DC subcarriers create zero bins and the pilot subcarriers form a spiky pattern, which cause errors in the occupancy monitoring. To alleviate this problem, these subcarriers ought to be discarded on the basis of their indices [46]. For instance, in the 802.11n/ac standard with a channel bandwidth of 20 MHz, the subcarriers are indexed from −32 to 32. The pilot subcarriers are identified by indices -28, -21, -14, -7, 7, 14, 21, and 28, while the DC/null subcarriers have an index range of −2 to 2. For occupancy detection, to retain only the data subcarriers in the CSI and remove the pilots and DC/null subcarriers, one can simply discard the pilot subcarriers (*i.e.*, indices -28, -21, -14, -7, 7, 14, 21, and 28), as well as DC/null subcarriers (*i.e.*, indices −2 to 2).[3] This process ensures that only the relevant data subcarriers are used for accurate occupancy detection.

[3] It is important to keep in mind that the index positions may vary for different channel widths, as elaborated in [46].

3.2. Filtering and feature extraction

CSI filtering

The indoor environment is subject to various unpredictable factors such as wall absorption (or penetration losses), room size, and the presence of obstacles, which can significantly increase the noise in the CSI data and result in errors during occupancy detection. To reduce the noise, filters in frequency and time domain such as the Butterworth filter and Median filter, respectively, are typically employed. However, these filters present some limitations. For instance, if a filter in the frequency domain such as the Butterworth filter is employed, noise leakage may occur from the stop-band into the pass-band due to the inherent delay of the fall-off feature [47]. Similarly, when a filter in the time domain such as the Median filter is used, significant distortion is caused to the CSI due to replacement of clean data (error-free CSI band) with noisy data (noisy CSI band) [48]. To overcome these limitations, we utilize the DWT as an in-band noise removal filter. The DWT decomposes the input signal into a multitude of wavelet basis functions. This transformation in the wavelet domain allows the signal to be represented in terms of coefficients of a time series. It is worth noting that the DWT parameters for noise removal such as cut-off threshold, wavelet type, and sampling rate should be carefully selected in order to maintain the necessary information on the occupant's activity in the CSI data. To ensure that the noise is removed from the in-band CSI data while preserving the occupants' daily activity information, we utilize the following Doppler frequency f_d formula to compute the cutoff threshold:

$$f_d = \frac{2v}{C} \times f_c \tag{1}$$

where v is the user velocity, C is the speed of light (*i.e.*, 3×10^8 m/s), and f_c is the carrier frequency of the commodity WiFi (*e.g.*, 2.4 GHz). Thus the f_d is 24 Hz and 80 Hz for walking (*i.e.*, 1.5 m/s) and running (*i.e.*, 5 m/s) respectively [49]. Using the maximum attainable Doppler frequency (*i.e.*, 80 Hz) as the cutoff threshold for DWT would retain all fluctuation in the CSI data below this frequency and remove noise levels above it [50].

Feature extraction

the data frame consists of multiple CSI subcarriers, represented as follows

$$\boldsymbol{H} = [H_1, H_2, \ldots, H_N]^T \text{ for } i = 1, 2, \ldots, N, \tag{2}$$

where H_i and N denote the individual ith subcarrier and total number of subcarriers, respectively. The ith subcarrier is defined as

$$H_i = |H_i| e^{j \sin\{\angle H_i\}}, \tag{3}$$

where in particular $|H_i|$ is the magnitude term and $\angle H_i$ is the phase responses of the subcarrier. In this work, we exploit the variation in the magnitude of the CSI's subcarrier when the communication link is obstructed by the user in the AOI. To do so, we extract the amplitude feature from each CSI subcarrier and then reduce the dimensionality of the CSI data in the sliding window W by applying Principal Component Analysis (PCA). It should be noted that the sliding window contains multiple data frames, and each data frame has several CSI subcarriers. The final feature of the CSI data is obtained by computing the first principal component, which is the maximum Eigen value of the Eigen vectors obtained from the correlation matrix of CSI in W.

The first principal component is an effective feature for occupancy monitoring because it captures the maximum variation in CSI data caused by motion. When there are no occupants in the AOI, the value of the first principal component is close to 1. However, in the presence of occupants performing any ADL in the AOI, its value changes dramatically between 0 and 1. As an example, we deliver a demonstration of occupancy detection with our feature value in Fig. 2. For this particular example, the CSI data was collected for 25 min, during which the occupant was present in the target area from 5 to 20 min.

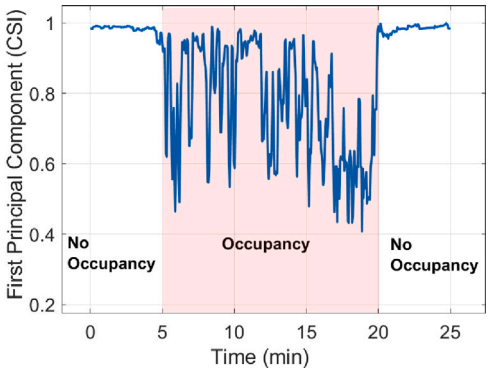

Fig. 2. Example of CSI feature with/without occupancy.

3.3. Occupancy detection method

The complex variation in indoor environments (due to, for example, room size, furniture arrangements, random activities of the individual, and absorption of walls) have a significant impact on the accuracy of occupancy detection. In light of these uncertain factors, conventional classification methods such as supervised machine learning or fixed thresholding may not be well-suited for scenarios with unpredictable variables (particularly in building environments, where room sizes, wall arrangements, and furniture layouts may change frequently and unpredictably). Therefore, we introduce a self-adaptive approach, which allows *WiSOM* to be flexible and compatible with any variation in the target setting.

3.3.1. Control chart approach

This method (also referred to as the Shewhart chart) is a stochastic process control method that is commonly applied in the industrial engineering discipline to produce products of high-quality [27]. In the control chart technique, the time-series quantity is regarded as stable when it stays within the control boundaries (defined by the control limit threshold). In contrast, the quantity is regarded as an outlier when it exceeds the control borders (or control limit). In our case, the stable state refers to the condition where there is no occupant in the target area, and the outlier state is the condition where an individual is present and causing the CSI to fluctuate. However, choosing a correct threshold for control limit to reliably identify the presence of occupant in a random indoor environment is quite challenging. Due to the complex and dynamic nature of indoor environments, a hard-coded threshold may be effective in one scenario, such as a small room with many obstacles, but not in other scenarios, *e.g.*, a large room with fewer obstacles. To make the control limit threshold self-adaptive to the changes in constant varying environments, we take advantage of the DBSCAN algorithm.

3.3.2. DBSCAN algorithm

The DBSCAN algorithm, a widely-used unsupervised machine-learning method, finds applications in various domains, including identifying charging zones for Electric Vehicles (EV) [51], determining local energy businesses [52], and identifying demand response (DR) among individual residential customers [53] *etc.* The default DBSCAN algorithm [26] requires two input parameters: ε and *MinPts*, which represent the center of a clusters of data points and the number of point in the cluster, respectively. The DBSCAN requires the following conditions to be met in order to form a cluster.

- The data point must be a core point; which means that a data point must occupy at least *MinPts* in its ε-neighborhood radius.

- The core points in the cluster must be density reachable; which means that any core point in the cluster can reach any other core point in that cluster, demonstrating symmetry density reachability. Moreover, it is also possible that any core point in the cluster can reach any other border point in that cluster, indicating asymmetry density reachability.
- If a data point fails to meet both of the above conditions, then it becomes an outlier.

Because of the random environmental factors, the CSI data points substantially change when the ambient environmental changes. Based on these environmental changes the distance between CSI data points (*i.e.*, feature value) fluctuates significantly. For instance, the distance between CSI data points will be significantly different in a small room compared to a large one, due to the difference in size and layout of the rooms. As a result, different ϵ and *MinPts* values would be required to identify the occupancy states in these two spaces. Typically, the value of ϵ in DBSCAN is determined using heuristic methods, such as finding the 'knee' [54] or the first 'valley' [26] in the k-distance graph. This type of 'knee' or 'valley' is the point at which the target cluster is separated from the outlier (or noise). Furthermore, *MinPts* value is set equal to the dimensions of data set [54]. However, manual selection of input parameters using this method is impractical because the 'knee' or 'valley' of CSI data points can frequently change due to variation in the indoor environment. In order to overcome this challenge, we have devised an approach that can automatically compute and adjust the *MinPts* and ϵ parameters. Our auto-tuning method comprises the following stages.

Auto-estimating the knee point: To determine the CSI data set's ϵ in arbitrary contexts, we employ the kneedle technique [30]. The fundamental goal of this method is to determine the data set's point which has the maximum curvature. This approach results in identifying a knee-point, which is the point in the data set located between data points that experience rapid changes (outliers or dispersed core points) and those that experience slower changes (congested core points). In the CSI data set, the knee-point obtained by the technique can be used as the bifurcation point that separates the cluster of non-occupant cases from the cluster of occupant cases. The steps for automatically estimating the 'knee' point are as follows:

1. First, the k-distance graph is transformed into negative concavity. This is done by flipping it by 180° about the origin. The endpoints of the flipped k-distance graph are connected so that the data set's overall characteristic is preserved. Furthermore, both x and y axes are normalized for maintaining the original data points trend, as depicted in Fig. 3(a).
2. The curve about the origin is rotated by θ° in a clockwise direction until the line connecting the ends intersects the x-axis.
3. The estimated 'knee' point for our CSI data points is the global maximum, which is determined from the peak of the curve, as depicted in Fig. 3(b).

Fine-tuning of the estimated parameters: The kneedle method yields a reliable knee point estimation when both the occupancy and non-occupancy states have adequate CSI data points. Nevertheless, there are two fundamental flaws in the standard kneedle method. First, severe multipath effects can occur in some indoor environments, such as small rooms with short inter-wall distances. Such effects can mask the mild ADL due to higher noise levels caused by multipath interference. Second, when any of the two states, *i.e.*, non-occupancy and occupancy, has short duration, the coarse parameters derived by the needle method will merge the data points from the shortest state with the longer one. As a result, a single cluster is generated for two distinct states. From this, we can infer two things: first, the ϵ value is sufficiently large and all of the data points meet the *MinPts* condition for the core point, thereby, every data point contained in the cluster is directly density reachable. Second, the value of *MinPts* is significantly less than the needed amount, whereby every data point becomes a core point and directly density reachable regardless of an accurate ϵ value.

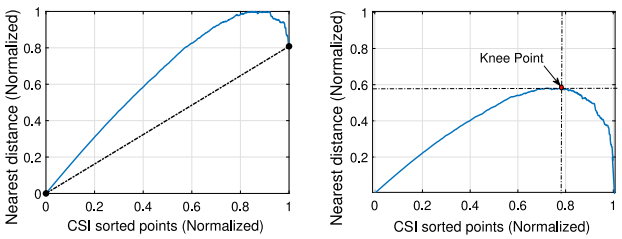

(a) Negative concavity of the sorted k-distance graph (normalized axis).

(b) The knee point located at the maximum curvature of the sorted data points.

Fig. 3. (a) Flipping of the sorted data points, (b) Finding the knee point.

To handle these issues, we present a technique for fine-tuning the input parameters (*i.e.*, ϵ estimated by the kneedle method and *MinPts*). First, *MinPts* is specified to be the same size as the number of dimensions in the dataset as in [54]. Then, the ϵ parameter is iteratively minimized whilst maximizing the *MinPts* until the two clusters (*i.e.*, occupancy and non-occupancy) are separate. Such ϵ and *MinPts* values that cause cluster separation are fine-tuned to classify the occupancy and non-occupancy clusters despite extreme multipath and brief ADL instances.

Determining the non-occupant data cluster: Fine-tuning facilitates the identification of two separate clusters, namely, non-occupancy and occupancy data clusters. As described in , CSI features associated with non-occupancy data are close to 1, while those related to occupancy data are in the range between 0.4 and 1, as illustrated in Fig. 2. Furthermore, in contrast to the occupancy case, which is highly variable and dispersed, the cluster produced from the non-occupancy case would have relatively congested data points. Based on these observations, the static cluster could be identified (that is, the one with the most congested core points and feature values that are near 1). We obtain the minimum feature value in the cluster using non-occupancy data and transfer it to the control chart. The control chart leverages this control limit threshold for differentiating between occupant and non-occupant states in real-time.

3.3.3. Synergistic unsupervised model

WiSOM offers a self-adaptive classification approach for occupancy detection. Thanks to the unsupervised learning, *WiSOM* does not require data labeling and training, and detect the occupant(s) in real-time.

To sum up, the auto-tuned DBSCAN algorithm gathers CSI data in batch mode and uses them to intelligently and precisely derive thresholds from the CSI's static clusters. This threshold is periodically updated in the control chart method, making it robust to any unanticipated changes in the target environment. As long as the instantaneous feature value of the CSI remains above this threshold in the control chart method, the state of the AOI is regarded as non-occupant. Conversely, if the value of the first principal component falls below such threshold, the state of the AOI is regarded as occupancy. By employing this method, *WiSOM* effectively distinguishes between occupant and non-occupant states based on the CSI measurements.

4. Implementation

Our testbed configuration is comprised of three device architecture: a transmitter device that sends data, a receiver (AP) which receives the

Table 1
Summary of experiments and data collection.

Experiment type	Occupant's activity(ies)	Use of indoor environment(s)	Duration of each data sample	Number of Data Samples
Impact of multipath	Moderate ADL	Varied spaces	30 min	150 data samples (3 scenarios)
ADL intensities	Varied ADL	Medium room	5 min	150 data samples (3 scenarios)
ADL instances	Moderate ADL	Medium room	10 min	100 data samples (2 scenarios)
Impact of temporal variations	Uncontrolled ADL	Medium room	120 min	40 data samples (4 scenarios)
Impact of wall losses	Moderate ADL	Medium room	10 min	100 data samples (4 scenarios)
Baseline Comparison	Moderate ADL	Varied spaces	10 min	125 data samples (5 scenarios)

data and acknowledges the reception,[4] and a sniffer, which overhears the communication between the transmitter and receiver. The transmitter in our testbed setting is a MacBook Pro laptop, which pings at varied throughput (40 ∼ 100 packets/sec) as in [55,56]. Notably, in smart buildings there are numerous WiFi-enabled IoTs, and they consistently exchange data with the APs. We believe that this much traffic is a sufficient assumption.[5] For the receiver, we use a couple of APs in our setting, including ASUS-AC2900, NETGEAR-N600, and TPLINK-AC1750 for the wireless Internet connection. They were all supporting dual-band connections. Finally, for the traffic sniffing (*i.e.*, pong traffic from the AP), we use a Raspberry (*RPi 3+*) for capturing the CSI. The default WLAN driver of *RPi 3+* does not support the monitoring mode and CSI extraction. To enable these features, we modify its driver by using the open-sourced GitHub repository of Nexmon [57]. The *RPi 3+* collects the CSI (OFDM modulated subcarriers) from the AP using UDP socket 5500 (for listening). The packet received on the listening port has source and destination IP addresses as 10.10.10.10 and 255.255.255.255 (*i.e.*, broadcasting IP), respectively. It is noteworthy that the CSI reception on multiple streaming is also possible if the receiving device supports MIMO However, in our case the *RPi 3+* only supported a single antenna with 2 dBi of gain. Therefore, the data was received on a single spatial stream.

We implemented the occupancy monitoring application for both real-time and offline modes. For the former implementation, we wrote a Python script for occupancy monitoring, and the *RPi 3+* was used to execute it via real-time CSI sniffing. In contrast, for the latter implementation, we transferred the CSI data to the MacBook via USB, and then tested the CSI data set on our occupancy monitoring program.

5. Evaluation

This section describes the experimental settings and the system's performance. We evaluated the robustness of *WiSOM* in a variety of environmental parameters, including (1) variation in indoor settings, (2) occupant activity intensities, (3) ADL instances, (4) temporal variation in CSI, (5) occupant detection behind single, and finally (6) its comparison with the recent baselines in real house scenario. Table 1 presents a brief overview of all our experimental setups. It includes details such as the type of experiment, the activities performed, the size of the environment, the duration, and the number of samples collected. Additional information regarding specific activities and environmental descriptions can be found in the details of the respective experiments.

5.1. Impact of multipath on WiSOM

In indoor environments, WiFi signals can encounter obstacles like walls and furniture, giving rise to additional signal paths known as multipath components. These multiple components, arriving at the receiver, can cause interference and distortion, leading to undesired fluctuations in the CSI measurements. Consequently, the estimation of CSI becomes contaminated, which can result in false positives in occupant detection within the AOI.

Experimental Setup. To assess the robustness of *WiSOM* in diverse multipath indoor environments, we consider three types of rooms: small, medium, and large with dimensions of 1.30 m × 3.15 m, 4m × 5m, and 8m × 8m, respectively. To make our experiment more realistic, we deliberately left the environmental conditions uncontrolled during the data collection process. To be precise, there was no control over the furniture arrangement, surrounding traffic (which could cause network jitter problem [28]), and people's motion in the vicinity of the room. The activity performed by the occupant was moderate (*i.e.*, walking in the room at a normal pace of 1.4 m/s). The data was collected for 30 min each time, in which the room was empty for the initial 10 min, and then occupied by the occupant for the latter time (*i.e.*, 10 ∼ 30 minutes).

Performance Evaluation. Figs. 4(a) and 4(b) show the performance of *WiSOM* in diverse multipath environments. The height of the bar plot shows the median value, whereas the lower and upper parts of the error bars represent the first and third quantiles, respectively. It is observed that *WiSOM* performs relatively worse in the small room compared to the other two rooms. This is due to the shorter inter-wall distance of the small room and the presence of certain scatters (such as furniture) in the target area, which further enhances the multipath effect. As a result of the enhanced multipath effect, errors can occur in the estimation of CSI, leading to inaccurate detection of occupants. This is demonstrated by the error bar of the small room, in Figs. 4(a) and 4(b) which show a higher variability for both detection rate and false alarm rate, respectively. On the contrary, the variability in the medium and large rooms is less severe. This indicates that the effect of the multipath decreases with an increase in the distance between the walls. Additionally, it is observed that the median detection rate in the medium room is around 98% with a false alarm rate of 2.43%, and the performance further improves in the large room, where the detection rate is 99% with a false alarm rate of only 1%.

5.2. Impact of ADL intensities on WiSOM

In this section, we present the results of the different intensities of Activities of Daily Living (ADL), which include activities performed with mild, moderate, and vigorous intensity levels. We provide details of the experimental setup and assessment procedures in the following.

Experimental Setup. To assess the robustness of *WiSOM* with activities of different intensities, we considered three types of ADLs: Mild, moderate, and vigorous. These three ADLs were conducted in a medium size room (4m × 5m) for 5 min each. The mild ADL consists of an individual wearing off a jacket and hanging it on a dressing stand and, then resting for some time on a chair. Such mild ADL has been conducted 8 times within 5 min. The moderate ADL consists of constant walking inside the room at a speed of 1.5 m/s. Finally, The vigorous activity involved the individual skipping in the room at an average rate of 3 skips/s.

[4] When the AP receives the ping packet, it responds back with a pong packet.

[5] In the extended version of this paper, we would like to evaluate *WiSOM*'s performance with variable traffic.

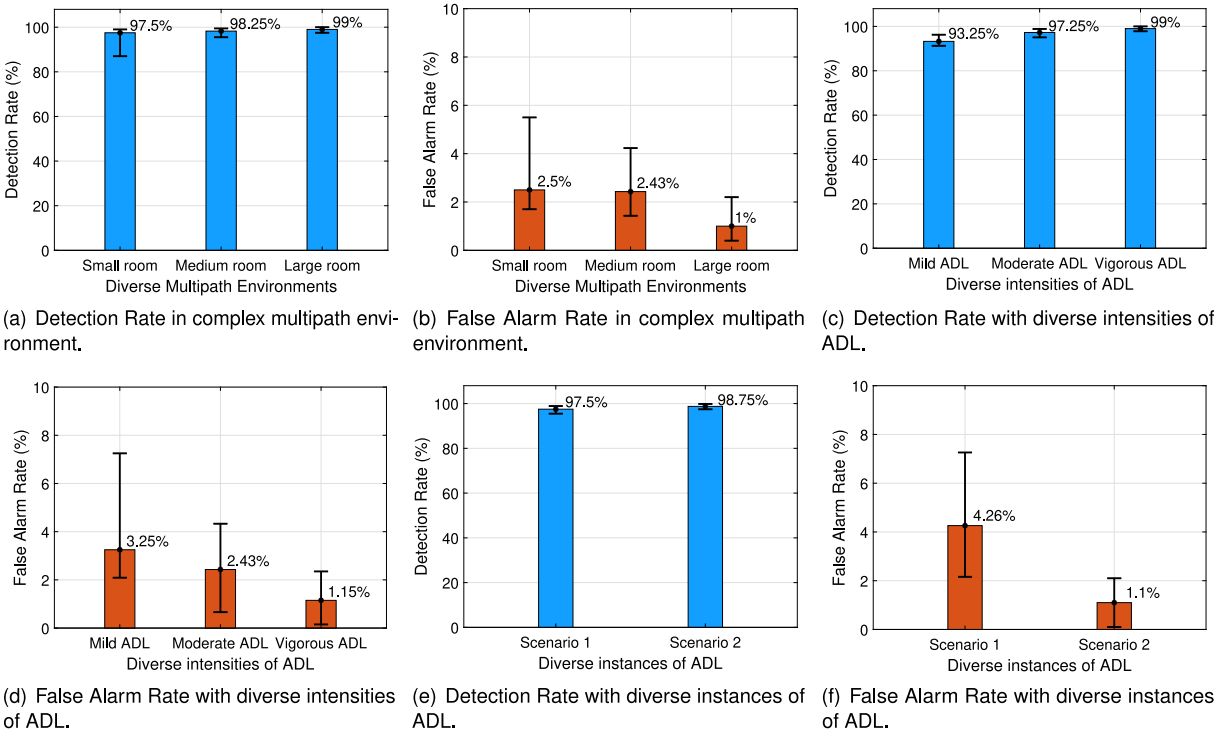

(a) Detection Rate in complex multipath environment.

(b) False Alarm Rate in complex multipath environment.

(c) Detection Rate with diverse intensities of ADL.

(d) False Alarm Rate with diverse intensities of ADL.

(e) Detection Rate with diverse instances of ADL.

(f) False Alarm Rate with diverse instances of ADL.

Fig. 4. Performance evaluation (a)~(b) in diverse multipath environment, (c)~(d) with variations of ADL intensities, and (e)~(f) with variations of ADL instances.

We collected 50 samples for each activity from a single individual at different times.

Performance Evaluation. The performance of *WiSOM* with diverse intensities of ADL is shown in Figs. 4(c) and 4(d). It is noteworthy that the mild ADL is sometimes masked by the multipath effect, therefore, it has a slightly lower detection rate (*i.e.*, around 93%). Similarly, the false alarm rate of the mild ADL is notably elevated compared to the moderate and vigorous ADL (*e.g.*, in some cases, we observed a false alarm rate of approximately 6.6% as depicted in the third quantile of the error bar). With an increase in the intensity of the ADL, the performance improves as higher intensity ADL can easily exceed the self-adaptive threshold and can be effectively distinguished from the no-activity cases. Notably, the detection rate for moderate activity reaches approximately 97%, while the false alarm rate is reduced to 2.43%. For the vigorous ADL case, the detection rate is around 99% with a false alarm rate further reduced to 1.15%.

5.3. Impact of ADL instances on WiSOM

The term "ADL instances" refers to the duration of time during which the occupant engages in specific activities of daily living. In the following sections, we discuss the experimental setup used to assess these ADL instances and evaluate their performance.

Experimental Setup. To assess the robustness of *WiSOM* with variable instances of ADL, we conducted the experiment in a medium-sized room with dimensions of 4m × 5m, and the duration was set to 10 min. Two scenarios were considered: In the first scenario, the room was occupied for three-quarters of the experiment's duration, which is equivalent to 7.5 min, and remained vacant for the remaining time. In the second scenario, we reversed the scenario, where the room was vacant for three-quarters of the experiment's duration, and then occupied for the remaining time. During the entire period (*i.e.*, 10 min) for each trial, the CSI data was continuously captured. Additionally, when the room was occupied the participant performed the moderate ADL described in Section 5.2.

Performance Evaluation. As evident from Fig. 4(e), Scenario 1 exhibits a marginally lower detection rate when compared to scenario 2. The reason behind this is that in scenario 1, there is a large cluster for the occupancy state and a small cluster for the non-occupancy state. As the control limit threshold is derived from the non-occupant cluster, which is smaller in scenario 1 case. In contrast, in scenario 2, there is a large amount of non-occupant data, and hence a large cluster for non-occupancy. This allows for a more precise computation of the control limit threshold in scenario 2. Consequently, scenario 2 slightly outperforms scenario 1. The comparison of both scenarios in terms of false alarm rate is illustrated in Fig. 4(f). It is clear that scenario 1 not only displays a higher median false alarm rate but also exhibits a marginally greater degree of variability in its error bars than depicted for scenario 2.

5.4. Impact of the temporal variations in CSI on WiSOM

Experimental Setup. To evaluate the temporal variation in the CSI measurement, we evaluated *WiSOM* across four different scenarios. In the first three scenarios, occupancy within the Area of Interest (AOI) alternated between occupied and unoccupied states over specified periods. In contrast, the fourth scenario represents a situation where the AOI remains entirely vacant, meaning there are no occupants in the AOI throughout the entire monitoring period. To provide a specific context, our experiment was conducted in a medium-sized room. For each scenario, we recorded CSI data over a span of two hours (or 120 min). In the first scenario, we started with the room being unoccupied for the first 20 min, followed by a period of occupancy for the next 20 min. This alternating pattern of vacancy and occupancy was continued until reaching the 120-minute mark, thereby resulting in a total of six instances of occupancy and non-occupancy throughout the duration. For the second scenario, we increased the period of occupancy and non-occupancy to 40 min, and repeated the experiment for 120 min. This ultimately resulted in a total of three instances of occupancy and non-occupancy throughout the duration. In the third scenario, we further increased the duration of both occupancy and non-occupancy periods to 60 min. This led to two instances of occupancy and non-occupancy within the 120-minute timeframe. Lastly, to assess

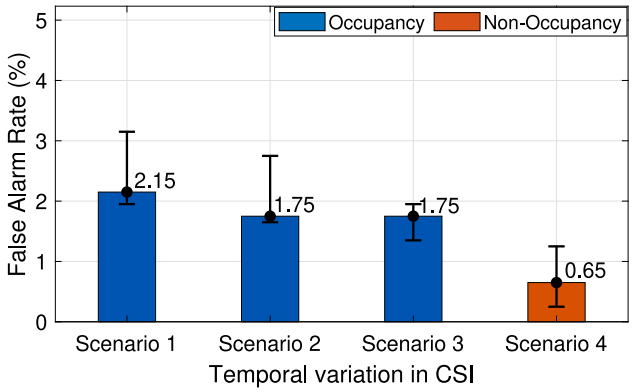

Fig. 5. False Alarm Rate obtained with temporal variations in CSI.

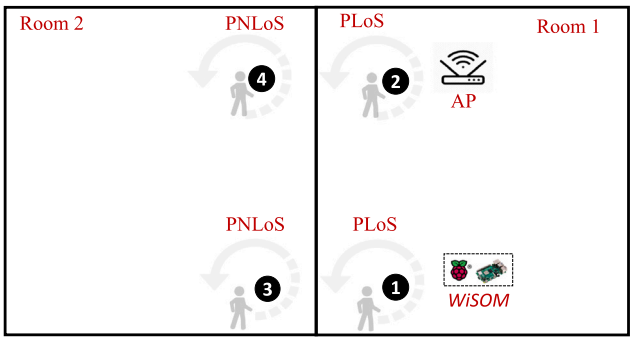

Fig. 6. Occupant in LoS and LNoS.

the ability of *WiSOM* to withstand the time-varying fluctuations of the CSI during non-occupant state, we conducted the fourth scenario, where the room remained completely vacant for the entire 120 min.

During the occupancy periods, we did not regulate the Activities of Daily Living (ADL) of the occupants. Users were free to engage in their normal routines while inside the room. This included activities such as reading a book while sitting on a rotating chair, walking around the room at a normal pace, or watching TV to prevent boredom, particularly in scenario 3, where the occupancy duration extended for an hour. Additionally, in each trial of the experiment, we intentionally relocated the rotating chair to a random position within the room. This was done to introduce variations in the CSI data, as a new chair position could result in different multipath reflection patterns, potentially inducing temporal variations in the CSI measurements. In total, we conducted 10 trials (each of 120 min) for each scenario.

Performance Evaluation. We deliver the false alarm rate of the CSI data collected for temporal variation in Fig. 5. The reason for solely considering the false alarm rate is to place greater emphasis on the occurrence of temporal variations, which are expected to indicate occupant detection in the static scenario (for non-occupancy states).

Interestingly, Fig. 5 shows that *WiSOM* is capable of effectively utilizing its self-adaptive feature to handle the temporal variations observed in CSI. In the occupancy scenarios (*i.e.*, scenario 1~3), we observed a slightly elevated false alarm rate in scenario 1. This increase is likely due to the regular switching between occupied and unoccupied states, along with the changing position of the chair within the room. The subsequent scenarios, specifically scenarios 2 and 3, display similar median false alarm rates. However, it is noteworthy that scenario 3 demonstrates reduced variability in its error bars compared to scenario 2. This is due to the fact that the extended period of non-occupancy allows for the collection of more CSI data (or the cluster formed from the static data points), enabling a more refined estimation of the control limit threshold. Consequently, this leads to a more accurate and intelligent distinction of the non-occupancy state. This effect becomes even more prominent in scenario 4, which is entirely a non-occupancy state, where we observe the false alarm rate dropping to below 1%.

5.5. Impact of wall losses on WiSOM

To thoroughly evaluate the effect of wall losses (or wall absorption loss), we performed an experiment involving a user walking in Line-of-Sight (LoS) to the *WiSOM* system, followed by the user moving behind a concrete wall with a thickness of 14 cm.

Table 2
LoS and NLoS occupancy evaluation.

Occupant's location (Loc)	Detection rate (%)	False alarm rate (%)
Loc 1	100%	0%
Loc 2	99.85%	0.45%
Loc 3	97.15%	3.1%
Loc 4	96.85%	4.75%

Experimental Setup. In this experimental setup, we evaluate the efficacy of *WiSOM* in detecting a person in LoS as well as a person in NLoS[6] as shown in Fig. 6. We acquire 10 min of CSI data at each position (marked by a solid black circle) during which the participant remains stationary for half of the time and engages in moderate ADL (i.e., walking) for the other half. At the locations 1 and 2, we collect data from the participant with a direct LoS; where, at location 1, the the participant is in close proximity to *WiSOM*, while, at location 2, the participant is located near the AP. We repeat the same consideration for the position of the participant with respect to the AP and *WiSOM* in locations 3 and 4, respectively. However, for these two locations, the participant is in NLoS condition.

Performance Evaluation. For this experimental setup, we observed that the performance of *WiSOM* did not vary significantly when the participant was moving in close proximity to either the *WiSOM* or the AP with a direct LoS. As the presence of a PLoS between the AP and *WiSOM* causes significant fluctuations in the wireless channel, which are reflected in the magnitude of the CSI. As a result, we have achieved higher detection rates with very low false alarm rates for detecting the occupant at these locations, as demonstrated in Table 2.

On the contrary, for locations 3 and 4, the impact of wall absorption is slightly more evident. Since the signal has to traverse through the walls and back, there is a two-way signal traversal attenuation. As a result, the signal's strength is partially absorbed by the walls, and this is reflected in the slightly lower performance behind the wall at both locations 3 and 4. Based on these results, it can be inferred that *WiSOM* exhibits resilience to single wall absorption in occupancy detection, with only a marginal impact on its performance.

5.6. Comparison with related WiFi occupancy monitoring systems

In this section, we conducted a comprehensive comparison between *WiSOM* and the most relevant and recent CSI-based occupancy monitoring solutions. We adapted these CSI-based occupancy monitoring

[6] Denoted by PLoS and PNLoS respectively in Fig. 6.

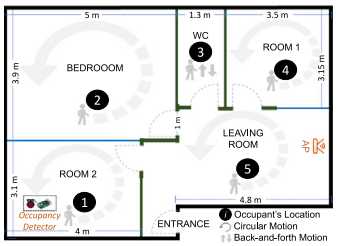

Occupant's activity at different locations of the house

(a) Activity of target individual at different locations (*Loc*) of the house.

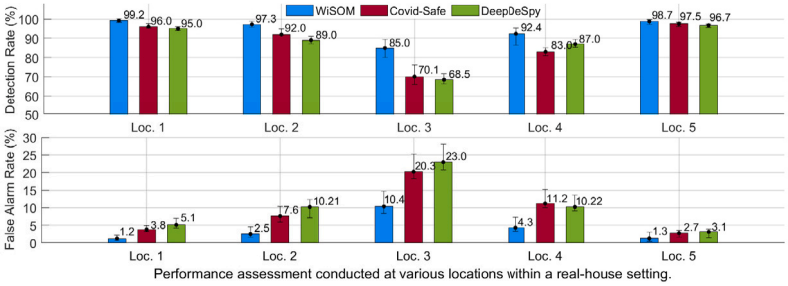

(b) *WiSOM*'s performance comparison with other SOTA systems.

Fig. 7. Real-house floor plane and comparison of *WiSOM* with the baseline techniques.

solutions to our specific real-house scenario shown in Fig. 7(a) and evaluated their performance. The selected scenario encompasses occupancy in both LoS and NLoS conditions, variable room sizes, and uncontrolled furniture arrangement. In the following, we provide a brief introduction to these systems and present a performance comparison with *WiSOM*.

Covid-Safe. The Covid-Safe [58] is intended for occupancy monitoring in epidemics such as COVID-19. It utilizes statistical features derived from CSI amplitude, such as mean, minimum value, maximum value, entropy, skewness, Median Absolute Difference (MAD), and standard deviations. These features are fed into a Support Vector Machine (SVM) classifier, which processes the data and makes predictions about the occupancy status.

DeepDeSpy. DeepDeSpy [59] is a solution designed to mitigate privacy invasion by focusing on the identification of occupants within a specific area. Its primary purpose is to detect the presence of individuals (or occupants) and subsequently predict the likelihood of a spy camera being present. They have developed a deep learning model consisting of a combination of a convolutional neural network (CNN) and a bidirectional long short-term memory (BiLSTM) network. The CNN is responsible for efficient and automatic feature learning, while the BiLSTM processes the CSI data in both backward and forward directions. This combination enables the detection of occupants in the AOI.

Experimental Setup. In this experimental setup, we conducted an in-the-wild study to assess the effectiveness of occupancy detectors in detecting a person located in different portions of a house. To accomplish this, we utilize a real-life house setting comprising five rooms, each with varying dimensions, as depicted in Fig. 7(a). The interior walls shown with blue line color represent drywall, while those in green color indicate single-brick walls (7.6 cm thick). The surrounding exterior walls represented by black color lines are concrete walls whose thickness is about 15.2 cm. The CSI data is collected for 10 min at each position, during which the user remains stationary for the first 5 min. Except for location 3, the user walks in a circular fashion for the last 5 min at all other positions. As the restroom, at location 3, offered limited space, we modified the walking pattern to back and forth motion instead of circular. The placement of the AP and occupancy detector was deliberately chosen at position 5 and 1, respectively, as their locations can be interchanged with other positions (such as *WiSOM* at position 2 or 3) without any significant effect on the results. Moreover, they were situated in different rooms to assess the impact of walls on their performance.

Performance Evaluation. In light of the above experimental settings, we conducted a comprehensive evaluation of every section of the house, including those with single or multiple walls away from the occupancy detectors, to assess their effectiveness in detecting the occupant.

As evident in Fig. 7(b), the superior performance of all occupancy detectors in detecting occupancy at locations (hereafter Loc.) 1 and 5 can be attributed to the presence of Line-of-Sight (LoS) conditions between the user and the detectors, and between the user and the AP, respectively. Such a condition allows the CSI to capture the resulting channel changes and utilize them for motion detection, leading to higher detection rates and lower false alarm rates. With a meticulous examination at the specified locations (*i.e.*, Loc. 1 and 5), *WiSOM* demonstrates a slight performance improvement compared to both Covid-Safe and DeepDeSpy, achieving a detection rate as high as 99.2% at Loc. 1, along with a mere 1.2% false alarm rate. Loc. 2 and 4 are both in Non-Line-of-Sight (NLoS) to the detectors, with Loc. 2 being close to the detectors and Loc. 4 being close to the Access Point (AP). However, in comparison to Location 4, the improved detection of occupancy at Loc. 2 can be attributed to two factors. Firstly, the room is in close proximity to the detectors. Secondly, the wall that separates rooms 1 and 2 is made of drywall, which exhibits a low absorption loss of 0.3 dB at 2.4 GHz, in contrast to the concrete walls that offer a higher absorption loss of 13.6 dB [60]. Similarly, Loc. 4, although situated farther from the detector, benefits from its close proximity to the AP. The CSI traveling from the AP to the detectors is influenced by the occupant's presence at Loc. 4, which is separated from Location 5 by a drywall. At both locations 2 and 4, *WiSOM* exhibits superior performance compared to its counterparts. Specifically, at Loc. 2, *WiSOM* achieves a detection rate that is 5.6% and 8.9% higher than Covid-Safe and DeepDeSpy, respectively. Similarly, at Loc. 4, *WiSOM* achieves a detection rate that is 10.7% and 6% higher than Covid-Safe and DeepDeSpy, respectively. At Loc. 3, the detectors' performance is adversely affected by three main factors. Firstly, the walls are made of bricks, causing higher absorption losses (6.45 dB of absorption loss [60]) compared to the drywall in previous cases. Secondly, the inter-wall distance is very short, leading to more severe multipath effects. Thirdly, the occupant at Loc. 3 is positioned behind multiple walls from the detector, further contributing to the decreased performance. Despite these challenging factors, *WiSOM* continued to outperform both Covid-Safe and DeepDeSpy, achieving a 19.2% and 21.5% higher detection rate (along with a lower false alarm rate).

6. Discussion and Future Work

We have evaluated the performance of *WiSOM* in diverse scenarios considering realistic factors such as room sizes, intensities of ADLs, duration of occupancy, temporal variations, and wall absorption. Overall, the results demonstrate the effectiveness of *WiSOM* for distinguishing occupancy and non-occupancy conditions with higher precision. It is noteworthy that the current work primarily focuses on evaluating the feasibility of occupancy detection using commodity WiFi devices. In our future research, we plan to explore the correlation between occupancy and energy consumption in a building. We would also like to acknowledge that there may be additional factors that need to be considered for specific environments and applications. Such factors are described below to identify potential directions for further improvement in future works.

Interference from the outdoor individuals: In this paper, we have focused on detecting the occupancy of users behind walls. However, a

careful reader may raise a concern about the possibility of detecting movements outside the AOI. We address this concern by noting that the exterior walls of buildings are typically made of concrete or bricks, which offer significant signal attenuation due to penetration losses. Therefore, any fluctuations caused by an outside user's movements would likely be minimal. However, in cases where the exterior walls are thin or outside users engage in vigorous activity, contamination of the CSI may occur. We plan to address this issue in detail in our future work and explore effective ways to mitigate the potential effects of outside individuals.

Number of occupants in an indoor environment: In our presented scenarios, we focused on the results for a single target individual. This was done in order to consider the worst-case scenario, as detecting the activity of a single occupant is generally more challenging compared to multiple users [58]. When multiple users are present, their combined activities cause greater changes in the CSI, making it easier to distinguish from non-occupant cases. However, since the number of occupants in an indoor environment can vary, with the average household size ranging from 2.3 to 5.5 individuals per household according to the literature [61,62], we plan to explore the impact of multiple users in our future work.

Impact of varied traffic sources: In the current setting, we generated a sufficient number of packets per second (40 ~ 100 packets/s) to ensure that our packet sniffing frequency was high enough to effectively monitor activity in the AOI. This is a realistic traffic rate in housing scenarios where WiFi-enabled IoT devices are consistently exchanging data with the internet [55,56]. However, it is also possible that in some houses, there are fewer WiFi-enabled IoT devices installed, which would result in lower traffic rates. In the future, we would like to evaluate the impact of these lower traffic rates on *WiSOM*'s performance, such as rates below 40 packets/s.

Presence of extraneous movements: There may be instances of extraneous movements in the AOI, such as the movement of curtains, pendulums, toys, and other similar objects, which could lead to temporal variation in CSI due to some non-human factors. However, these are typically micromovements and would likely result in minimal false positives. In our future work, we also plan to investigate ways to differentiate between extraneous movements and actual occupancy movements.

Fully dynamic ADL: In the evaluation of ADL with dynamic instances, we did not consider a scenario where the ADL is fully dynamic, as *WiSOM* requires a minimum static duration to update the online threshold. However, it is unlikely to have a fully dynamic scenario where a person is consistently moving without stopping. In such cases, we use a default static threshold value to handle the situation. This default threshold is then updated to a quasi-optimal value when *WiSOM* detects a sedentary behavior from the user (*i.e.*, activity lasting for at least 2 s).

7. Conclusion

In this work, we propose a self-adaptive system that utilizes off-the-shelf WiFi for occupancy monitoring in smart buildings. The system aims to address the issue of energy wastage by optimizing energy consumption based on occupancy detection. *WiSOM* does not require data labeling or pre-training and works robustly in real-time. Furthermore, *WiSOM* is robust to the complex variations found in indoor environments, such as variations in space size, ADLs with different intensities and instances, temporal variation in the CSI, and the impact of wall absorption. In various indoor settings, *WiSOM* demonstrated a high average detection rate of 98.25%. It also performed well with diverse ADL intensities and instances, achieving a detection rate of 96.5% and 98.1%, respectively. Additionally, the system was tested in both lab and real-home environments to assess the impact of wall losses. In NLoS scenarios, the average accuracy was 97%, which was 2.9% lower than in LoS scenarios. *WiSOM* was also robust to temporal variations in CSI, with a false alarm rate of less than 2%. In real-house scenarios with varying room dimensions, NLoS conditions, and wall occlusions, *WiSOM* demonstrated a performance gain of up to 21% compared to recent CSI-based occupancy detection systems.

We acknowledge certain limitations in our current system. The reliance on WiFi signals renders our system susceptible to extraneous movements, particularly if walls are constructed from less dense materials like wood or plaster. This could result in the detection of external movements, potentially leading to higher false motion detection. Furthermore, in some rare cases, *WiSOM* might not be able to adjust its threshold appropriately, for instance, in areas with constant movement. In such a case, it depends on a pre-trained motion detection threshold, which can occasionally lead to false results. External factors like varied traffic sources and extraneous motion can also impact detection accuracy. These limitations are detailed in Section 6, and addressing them will be a focus of our future work.

CRediT authorship contribution statement

Muhammad Salman: Conceptualization, Data curation, Formal analysis, Methodology, Project administration, Software, Visualization, Writing – original draft, Writing – review & editing. **Lismer Andres Caceres-Najarro:** Resources, Visualization, Writing – original draft. **Young-Duk Seo:** Investigation, Project administration. **Youngtae Noh:** Conceptualization, Funding acquisition, Project administration, Resources, Supervision.

Declaration of competing interest

The authors declare the following financial interests/personal relationships which may be considered as potential competing interests: Youngtae Noh reports financial support was provided by Korea Institute of Energy Technology. If there are other authors, they declare that they have no known competing financial interests or personal relationships that could have appeared to influence the work reported in this paper.

Data availability

The authors do not have permission to share data.

Acknowledgments

This study received partial support from the Basic Science Research Program by the National Research Foundation of Korea (NRF), funded by the Ministry of Education under grant numbers NRF-2020R1A4A1018774, NRF-2021M3A9E4080780, and NRF-2021R1I1A1A01041257, as well as from the Ministry of Trade, Industry, and Energy (MOTIE) under grant number RS-2023-00236325.

References

[1] Roser M, Ritchie H, Ortiz-Ospina E, Rodés-Guirao L. World population growth. Our World Data 2013.
[2] D'Oca S, Hong T, Langevin J. The human dimensions of energy use in buildings: A review. Renew Sustain Energy Rev 2018;81:731–42.
[3] Meyers RJ, Williams ED, Matthews HS. Scoping the potential of monitoring and control technologies to reduce energy use in homes. Energy Build 2010;42(5):563–9.
[4] Stauffer NW. Reducing wasted energy in commercial buildings. 2013, URL https://tinyurl.com/2d2mkccx.
[5] Hu M, Xiao F. Quantifying uncertainty in the aggregate energy flexibility of high-rise residential building clusters considering stochastic occupancy and occupant behavior. Energy 2020;194:116838.
[6] Andrews J, Kowsika M, Vakil A, Li J. A motion induced passive infrared (PIR) sensor for stationary human occupancy detection. In: 2020 IEEE/ION position, location and navigation symposium. PLANS, IEEE; 2020, p. 1295–304.
[7] Dodier RH, Henze GP, Tiller DK, Guo X. Building occupancy detection through sensor belief networks. Energy Build 2006;38(9):1033–43.

[8] Hong J, Tomii S, Ohtsuki T. Cooperative fall detection using Doppler radar and array sensor. In: 2013 IEEE 24th annual international symposium on personal, indoor, and mobile radio communications. IEEE; 2013, p. 3492–6.

[9] Narayana S, Prasad RV, Rao VS, Prabhakar TV, Kowshik SS, Iyer MS. PIR sensors: Characterization and novel localization technique. In: Proceedings of the 14th international conference on information processing in sensor networks. 2015, p. 142–53.

[10] Hammoud A, Deriaz M, Konstantas D. Ultrasense: A self-calibrating ultrasound-based room occupancy sensing system. Procedia Comput Sci 2017;109:75–83.

[11] Jin M, Bekiaris-Liberis N, Weekly K, Spanos CJ, Bayen AM. Occupancy detection via environmental sensing. IEEE Trans Autom Sci Eng 2016;15(2):443–55.

[12] Calì D, Matthes P, Huchtemann K, Streblow R, Müller D. CO2 based occupancy detection algorithm: Experimental analysis and validation for office and residential buildings. Build Environ 2015;86:39–49.

[13] Yasuda T, Yonemura S, Tani A. Comparison of the characteristics of small commercial NDIR CO2 sensor models and development of a portable CO2 measurement device. Sensors 2012;12(3):3641–55.

[14] Quan VM, Gupta GS, Mukhopadhyay S. Review of sensors for greenhouse climate monitoring. In: 2011 IEEE sensors applications symposium. IEEE; 2011, p. 112–8.

[15] Cui Z, Sun Y, ce Gao D, Ji J, Zou W. Computer-vision-assisted subzone-level demand-controlled ventilation with fast occupancy adaptation for large open spaces towards balanced IAQ and energy performance. Build Environ 2023;239:110427. http://dx.doi.org/10.1016/j.buildenv.2023.110427, URL https://www.sciencedirect.com/science/article/pii/S0360132323004547.

[16] Saffari A, Tan SY, Katanbaf M, Saha H, Smith JR, Sarkar S. Battery-free camera occupancy detection system. In: Proceedings of the 5th international workshop on embedded and mobile deep learning. 2021, p. 13–8.

[17] Hu S, Wang P, Hoare C, O'Donnell J. Building occupancy detection and localization using CCTV camera and deep learning. IEEE Internet Things J 2023;10(1):597–608. http://dx.doi.org/10.1109/JIOT.2022.3201877.

[18] Wang J, Huang J, Feng Z, Cao S-J, Haghighat F. Occupant-density-detection based energy efficient ventilation system: Prevention of infection transmission. Energy Build 2021;240:110883.

[19] Zou H, Zhou Y, Yang J, Spanos CJ. Device-free occupancy detection and crowd counting in smart buildings with WiFi-enabled IoT. Energy Build 2018;174:309–22.

[20] Zou H, Zhou Y, Yang J, Gu W, Xie L, Spanos C. Freedetector: Device-free occupancy detection with commodity wifi. In: 2017 IEEE international conference on sensing, communication and networking. IEEE; 2017, p. 1–5.

[21] Yang J, Zou H, Jiang H, Xie L. Device-free occupant activity sensing using WiFi-enabled IoT devices for smart homes. IEEE Internet Things J 2018;5(5):3991–4002.

[22] Soltanaghaei E, Kalyanaraman A, Whitehouse K. Peripheral wifi vision: Exploiting multipath reflections for more sensitive human sensing. In: Proceedings of the 4th international on workshop on physical analytics. 2017, p. 13–8.

[23] Salman M, Son J-H, Choi D-W, Lee U, Noh Y. DARCAS: Dynamic association regulator considering airtime over SDN-enabled framework. IEEE Internet Things J 2022;9(20):20719–32.

[24] Abolhassani SS, Zandifar A, Ghourchian N, Amayri M, Bouguila N, Eicker U. Improving residential building energy simulations through occupancy data derived from commercial off-the-shelf Wi-Fi sensing technology. Energy Build 2022;272:112354.

[25] Salman M, Soe Y-D, Noh Y. WiFi-enabled occupancy monitoring in smart buildings with a self-adaptive mechanism. In: Proceedings of the 38th ACM/SIGAPP symposium on applied computing. 2023, p. 759–62.

[26] Ester M, Kriegel H-P, Sander J, Xu X, et al. A density-based algorithm for discovering clusters in large spatial databases with noise. In: Kdd. Vol. 96. no. 34. 1996, p. 226–31.

[27] Tague N. The quality toolbox, ASQ (american society for quality). Quality Press; 2004.

[28] Salman M, Dao N, Lee U, Noh Y. CSI: DeSpy: Enabling effortless Spy camera detection via passive sensing of user activities and bitrate variations. Proc ACM Interact Mob Wearable Ubiquitous Technol 2022;6(2):1–27.

[29] Piselli C, Pisello AL. Occupant behavior long-term continuous monitoring integrated to prediction models: Impact on office building energy performance. Energy 2019;176:667–81.

[30] Satopaa V, Albrecht J, Irwin D, Raghavan B. Finding a" kneedle" in a haystack: Detecting knee points in system behavior. In: 2011 31st international conference on distributed computing systems workshops. IEEE; 2011, p. 166–71.

[31] Lee H, Ahn CR, Choi N. The impacts of CSI temporal variations on CSI-based occupancy monitoring systems: An exploratory study. In: Proceedings of the 7th ACM international conference on systems for energy-efficient buildings, cities, and transportation. 2020, p. 278–81.

[32] Lee DT, Yamamoto A. Wavelet analysis: Theory and applications. Hewlett Packard J 1994;45:44.

[33] Xu Y, Weaver JB, Healy DM, Lu J. Wavelet transform domain filters: A spatially selective noise filtration technique. IEEE Trans Image Process 1994;3(6):747–58.

[34] Jocher G, Stoken A, Borovec J, NanoCode012, Chaurasia A, TaoXie, et al. Ultralytics/yolov5: v5.0 - YOLOv5-P6 1280 models, AWS, supervise.ly and YouTube integrations. 2021, https://github.com/ultralytics/yolov5/releases/tag/v5.0.

[35] Mahmud A, Dhrubo EA, Ahmed SS, Chowdhury AH, Hossain MF, Rahman H, et al. Energy conservation for existing cooling and lighting loads. Energy 2022;255:124588.

[36] Han Z, Gao RX, Fan Z. Occupancy and indoor environment quality sensing for smart buildings. In: 2012 IEEE international instrumentation and measurement technology conference proceedings. 2012, p. 882–7. http://dx.doi.org/10.1109/I2MTC.2012.6229557.

[37] Balaji B, Xu J, Nwokafor A, Gupta R, Agarwal Y. Sentinel: Occupancy based HVAC actuation using existing WiFi infrastructure within commercial buildings. In: Proceedings of the 11th ACM conference on embedded networked sensor systems. 2013, p. 1–14.

[38] Cecchet E, Acharya A, Molom-Ochir T, Trivedi A, Shenoy P. WiFiMON: A mobility analytics platform for building occupancy monitoring and contact tracing using WiFi sensing. In: Proceedings of the 18th conference on embedded networked sensor systems. 2020, p. 792–3.

[39] Depatla S, Muralidharan A, Mostofi Y. Occupancy estimation using only WiFi power measurements. IEEE J Sel Areas Commun 2015;33(7):1381–93.

[40] Longo E, Redondi AE, Cesana M. Accurate occupancy estimation with WiFi and bluetooth/BLE packet capture. Comput Netw 2019;163:106876.

[41] Xu C, Firner B, Moore RS, Zhang Y, Trappe W, Howard R, et al. SCPL: Indoor device-free multi-subject counting and localization using radio signal strength. In: Proceedings of the 12th international conference on information processing in sensor networks. 2013, p. 79–90.

[42] Caceres-Najarro LA, Song I, Kim K. Fundamental limitations and state-of-the-art solutions for target node localization in WSNs: A review. IEEE Sens J 2022.

[43] Yang Z, Zhou Z, Liu Y. From RSSI to CSI: Indoor localization via channel response. ACM Comput Surv 2013;46(2):1–32.

[44] Zou H, Zhou Y, Yang J, Gu W, Xie L, Spanos C. Multiple kernel representation learning for WiFi-based human activity recognition. In: 2017 16th IEEE international conference on machine learning and applications. IEEE; 2017, p. 268–74.

[45] Bhartia A, Chen Y-C, Rallapalli S, Qiu L. Harnessing frequency diversity in Wi-Fi networks. In: Proceedings of the 17th annual international conference on mobile computing and networking. 2011, p. 253–64.

[46] Gast MS. 802.11 Ac: A survival guide: Wi-Fi at Gigabit and beyond. O'Reilly Media, Inc; 2013.

[47] Palipana S, Rojas D, Agrawal P, Pesch D. FallDeFi: Ubiquitous fall detection using commodity Wi-Fi devices. Proc ACM Interact Mob Wearable Ubiquitous Technol 2018;1(4):1–25.

[48] Mehta R, Aggarwal NK. Comparative analysis of median filter and adaptive filter for impulse noise–a review. Int J Comput Appl 2014;975:8887.

[49] BBCcom. Everyday motion. 2020, URL https://tinyurl.com/2humk9u2.

[50] Ram SS, Li Y, Lin A, Ling H. Doppler-based detection and tracking of humans in indoor environments. J Franklin Inst B 2008;345(6):679–99.

[51] Faustino FJ, Lopes JC, Melo JD, Sousa T, Padilha-Feltrin A, Brito JA, et al. Identifying charging zones to allocate public charging stations for electric vehicles. Energy 2023;283:128436.

[52] González FF, Webb J, Sharmina M, Hannon M, Braunholtz-Speight T, Pappas D. Local energy businesses in the United Kingdom: Clusters and localism determinants based on financial ratios. Energy 2022;239:122119.

[53] Shi R, Jiao Z. Individual household demand response potential evaluation and identification based on machine learning algorithms. Energy 2023;266:126505.

[54] Hahsler M, Piekenbrock M, Doran D. Dbscan: Fast density-based clustering with R. J Stat Softw 2019;91(1):1–30.

[55] Nguyen-An H, Silverston T, Yamazaki T, Miyoshi T. IoT traffic: Modeling and measurement experiments. IoT 2021;2(1):140–62.

[56] Sharma A, Li J, Mishra D, Batista G, Seneviratne A. Passive WiFi CSI sensing based machine learning framework for COVID-safe occupancy monitoring. In: 2021 IEEE international conference on communications workshops. IEEE; 2021, p. 1–6.

[57] Schulz M, Wegemer D, Hollick M. Nexmon: The C-based firmware patching framework. 2017, URL https://nexmon.org.

[58] Li J, Sharma A, Mishra D, Batista G, Seneviratne A. COVID-safe spatial occupancy monitoring using OFDM-based features and passive WiFi samples. ACM Trans Manag Inf Syst 2021;12(4). http://dx.doi.org/10.1145/3472668.

[59] Dao D, Salman M, Noh Y. DeepDeSpy: A deep learning-based wireless spy camera detection system. IEEE Access 2021;9:145486–97. http://dx.doi.org/10.1109/ACCESS.2021.3121254.

[60] Safaai-Jazi A, Riad SM, Muqaibel A, Bayram A. Ultra-wideband propagation measurements and channel modeling. In: Report on through-the-wall propagation and material characterization. 2002.

[61] Steemers K, Yun GY. Household energy consumption: A study of the role of occupants. Build Res Inform 2009;37(5–6):625–37.

[62] United Nations. Household size and composition. 2022, URL https://tinyurl.com/2p983dzh.